Coexistence of forest and savanna in an Amazonian area from a geological perspective

D.F. Rossetti, S. Almeida, D.D. Amaral, C.M. Lima & L.C.R. Pessenda

Abstract

Question: How can the coexistence of savanna and forest in Amazonian areas with relatively uniform climates be explained?

Location: Eastern Marajó Island, northeast Amazonia, Brazil.

Methods: The study integrated floristic analysis, terrain morphology, sedimentology and $\delta^{13}C$ of soil organic matter. Floristic analysis involved rapid ecological assessment of 33 sites, determination of occurrence, specific richness, hierarchical distribution and matrix of floristic similarity between paired vegetation types. Terrain characterization was based on analysis of Landsat images using 4(R), 5(G) and 7(B) composition and digital elevation model (DEM). Sedimentology involved field descriptions of surface and core sediments. Finally, radiocarbon dating and analysis of $\delta^{13}C$ of soil profile organic matter and natural ecotone forest-savanna was undertaken.

Results: Slight tectonic subsidence in eastern Marajó Island favours seasonal flooding, making it unsuitable for forest growth. However, this area displays slightly convex-up, sinuous morphologies related to paleochannels, covered by forest. *Terra-firme* lowland forests are expanding from west to east, preferentially occupying paleochannels and replacing savanna. Slack, running water during channel abandonment leads to disappearance of *varzea/* gallery forest at channel margins. Long-abandoned channels sustain continuous *terra-firme* forests, because of longer times for more species to establish. Recently abandoned channels have had less time to become sites for widespread tree development, and are either not vegetated or covered by savanna.

Rossetti, D.F. (corresponding author, rossetti@dsr.inpe.br): Instituto Nacional de Pesquisas Espaciais-OBT/DSR, Rua dos Astronautas 1758 CP 515, 12245-970 São José dos Campos, SP, Brazil

Almeida, S. & Amaral, D.D.: Museu Paraense Emílio Goeldi, Coordenação de Botânica, Av. Perimetral 1901 CP 399, 66077-530 Belém, PA- Brazil

Lima, C.M. & Pessenda, L.C.R.: Universidade de São Paulo, Laboratório de ^{14}C, Avenida Centenário 303, 13416000 Piracicaba, SP - Brazil.

Conclusion: Landforms in eastern Marajó Island reflect changes in the physical environment due to reactivation of tectonic faults during the latest Quaternary. This promoted a dynamic history of channel abandonment, which controlled a set of interrelated parameters (soil type, topography, hydrology) that determined species location. Inclusion of a geological perspective for paleoenvironmental reconstruction can increase understanding of plant distribution in Amazonia.

Keywords: Amazonia; Geological history; Paleolandscape; Plant distribution; Quaternary; $\delta^{13}C$ isotope.

Nomenclature: Cronquist (1981).

Introduction

Many studies have highlighted the importance of climate on species distribution (Pearson & Dawson 2003; ter Steege et al. 2003; Huntley et al. 2004), however, Amazonian species do not respond only to climate changes (Haffer 1990; Ayres & Clutton-Brock 1992), and a wider range of environmental parameters should therefore be considered (Bush 1994; Tuomisto et al. 1995; Bonaccorso et al. 2006; Coudun et al. 2006). Numerous hypotheses have been formulated in this regard, considering the influence of topography (Tuomisto et al. 1995; Vormisto et al. 2004), soil (Tuomisto & Ruokolainen 1994) and geology (Räsänen et al. 1990; Van der Hammen et al. 1992). A crucial step to understand Amazonian biodiversity is to identify the environmental parameters that, in addition to climate, might have determined the distribution of modern species. Of particular interest is the coexistence of forest and savanna in many Amazonian areas, which is unlikely to respond only to climatic changes. Patches of savanna within the Amazonian dense forest have been interpreted as relics of increased aridity in the late Pleistocene (Ledru et al. 2006) and early to mid-Holocene (Pessenda et al. 1998; Freitas et al. 2001).
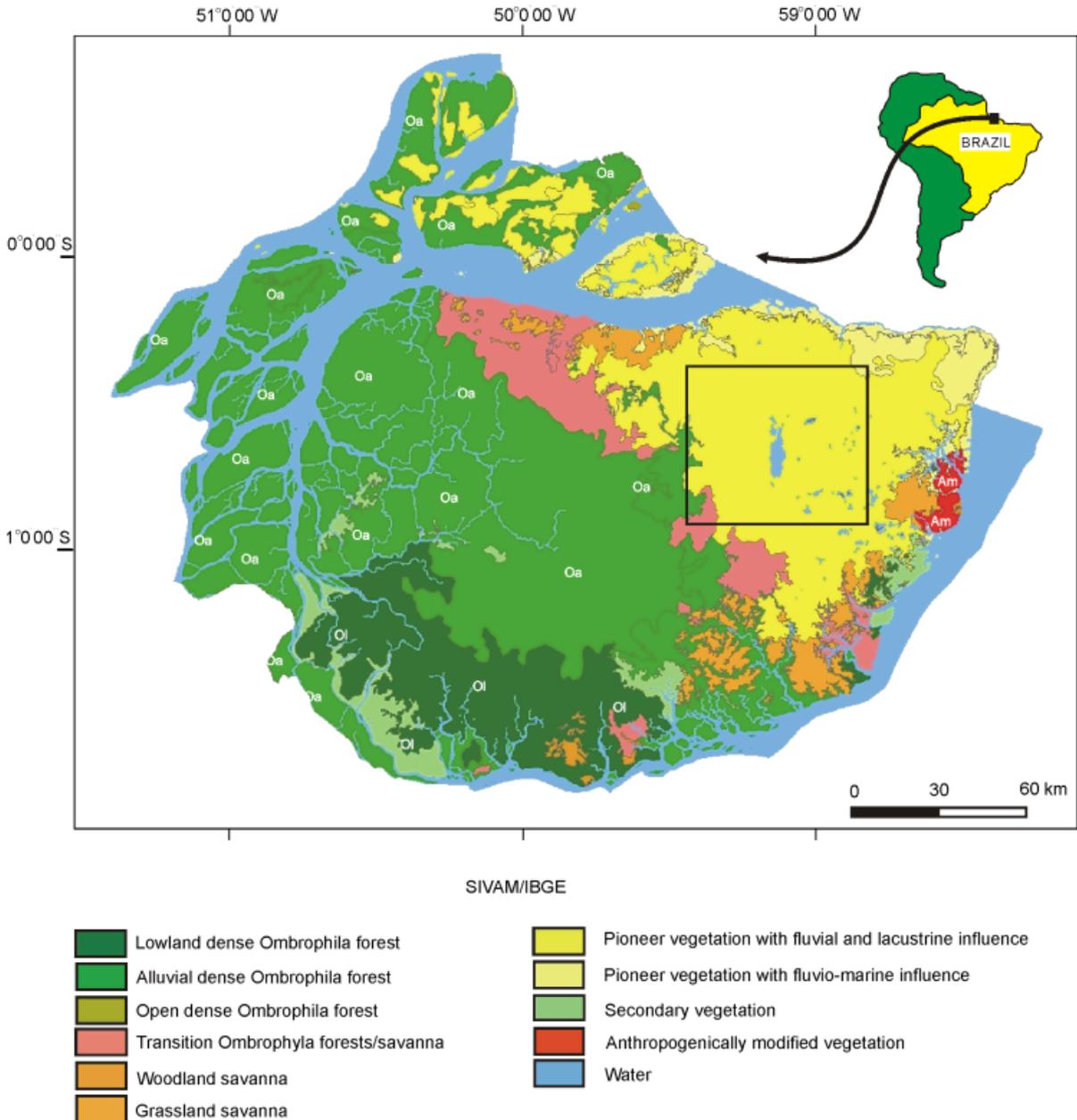
The goal of this study is to introduce an alternative model based on landform evolution to explain the coexistence of forest and savanna in

Fig. 1. Location map of the study area in Marajó Island, northern Brazil, with distribution of vegetation types (based on SIVAM/IBGE). Inside box locates the study area.

an Amazonian area. The example discussed herein derives from eastern Marajó Island, located at the mouth of the Amazon River. The eastern side of this island sustains a mosaic of savanna and forest, while dense forest prevails on its western side. This work focuses on the relationship between these contrasting vegetation types and the geological characteristics of the study area. The aim is to determine the influence of geological history on plant distribution in the Amazonian lowland.

Physiography and Geologic Framework

The study area (Fig. 1) is characterized by a tropical climate, with mean annual temperature of 28°C and precipitation of 2500 to 3000 mm yr^{-1}. Vegetation types consist of two sharply-bounded groups: savanna (or *campo*), which consists mostly of grassland, *cerrado* (Miranda & Carneiro 1994) and savanna woodland in the eastern side of the island; and dense tropical *Ombrophyla* forest

(e.g. Bastos 1984; Pires & Prance 1985; Henderson et al. 1991;Fig. 1) including *terra-firme* and seasonally flooded *varzea*/gallery forests in the western side of the island. The *campos* from eastern Marajó, where the study area is located, are flooded during rainy seasons for a period of 3 to 4 months. A few, usually elongated, areas above high-water level are sites suitable for tree growth. Soils are dominated by poorly drained, hydromorphic gleysols (Aquept, USDA Soil Taxonomy 1999), with a few podzols (Udult) (RADAM 1974). *Terra-firme* forests have distinct oligotrophic, acidic, moderately drained latosols (Udox) with a sandy or sandy-muddy texture, while mosaics of *terra-firme* forest and savanna have yellow latosols (Udox). Areas dominated by grassland savanna might lack soil horizon, when mud settling is still taking place, either during flooding or all year round in depressed areas where lakes of various sizes are present.

Geologically, western Marajó Island is inserted in the Limoeiro Sub-Basin of the Marajó Graben System, while its eastern side is within the Pará Platform. The surface of this island is covered mostly by pos-Barreiras deposits of Pleistocene and Holocene age, in addition to a narrow belt of Miocene deposits of the Barreiras Formation in its easternmost edge. Quaternary deposits were formed within a tectonically controlled N/NW-S/SE orientated paleovalley (Rossetti & Valeriano 2007; Rossetti et al. 2007). According to these authors, this valley was fed by a paleo-Tocantins River. The abandonment of this river left numerous paleochannels that are still preserved in Marajó landscape (e.g. Radam 1974; Porsani 1981).

Methods

The present investigation integrated floristic composition, terrain morphology, sedimentology and $\delta^{13}C$ of organic matter from soil profiles. The floristic survey consisted of a rapid ecologic evaluation (REE) (Sayre et al. 2000). Thirty-three sites were established to record the distribution of the various vegetation patterns. Descriptions were made within a 50-m radius in each site, inventorying all vascular plant species, and annotating species occurrence as follows: (1) Abundant: large populations forming monospecific patches or aggregates; (2) Common: numerous but without patches or aggregates; and 3. Occasional or rare for random or infrequent species. The Cronquist (1981) classification system was applied to define plant family names. The studied sites were grouped into eight

phytophysiognomic types, following the macrophysionomies of SIVAM/IBGE (Fig. 1), with a few modification aiming to preserve terms commonly used by local researchers (e.g. Bastos 1984; Pires & Prance 1985; Henderson et al. 1991). The phytophysiognomies were assigned upper cases for Forest (F) and Savanna (S), followed by low cases to specify vegetation type (e.g. Sw = woodland savanna). Statistical processing was applied with the software PC-ORD for windows (McCune & Mefford 1997).

Terrain characterization was based on interpretation of Landsat 5-TM (Ref. 224-060 and 225-061, INPE) and Landsat 7-ETM+(Ref. 223-060 and 223-061, GLCF) images, acquired in August 2001. A 4(R), 5(G) and 7(B) band composition scheme, processed with the software SPRING, provided a good view of the geomorphic features of interest for this study. The geomorphic characterization was completed with application of digital elevation model (DEM) derived from the Shuttle Radar Topography Mission (SRTM).

The field study consisted of morphological characterization to confirm the landforms previously recognized on the images, added to descriptions of sediments at the surface of the various phytophysiognomies. At three localities this analysis was accompanied by core descriptions obtained with a shallow percussion drilling system (RKS-Robotic Key System; COBRA mk1 (COBRA Directional Drilling Ltd, UK). Three continuous cores of 5-cm diameter and up to 18-m long (Fig. 2) were obtained on the large (T1 and T3) and narrow (T2) paleochannels described herein, and several other drillings were made on nearby floodplain areas. Descriptions included definition of sedimentary facies based on lithology, texture, structure and vertical facies relationships.

Carbon isotope (^{12}C, ^{13}C) analyses of organic matter were performed at three localities (see localities 1, 3 and 4 in Fig. 2). Samples of sediment units (85) were collected along shallow manual drillings and trenches at 10-cm intervals. Grain size analyses were performed using dry sieving. After pre-treatment (Pessenda et al. 1996), the samples were analysed at the Stable Isotope Laboratory of CENA/USP (São Paulo, Brazil). $\delta^{13}C$ values were also obtained from 14 modern plant species categorized as abundant in each sampling site. Results are expressed as $\delta^{13}C$ with respect to PDB (Peedee Belemnite Standard) standard using the conventional $\delta(‰)$ notation $\delta^{13}C$ $(‰) = [(R_{sample}/R_{standard}) - 1]\,1000$, where R_{sample} and $R_{standard}$ are the $^{13}C/^{12}C$ ratio of the sample and standard, respectively. Analytical precision is $\pm 0.2‰$.
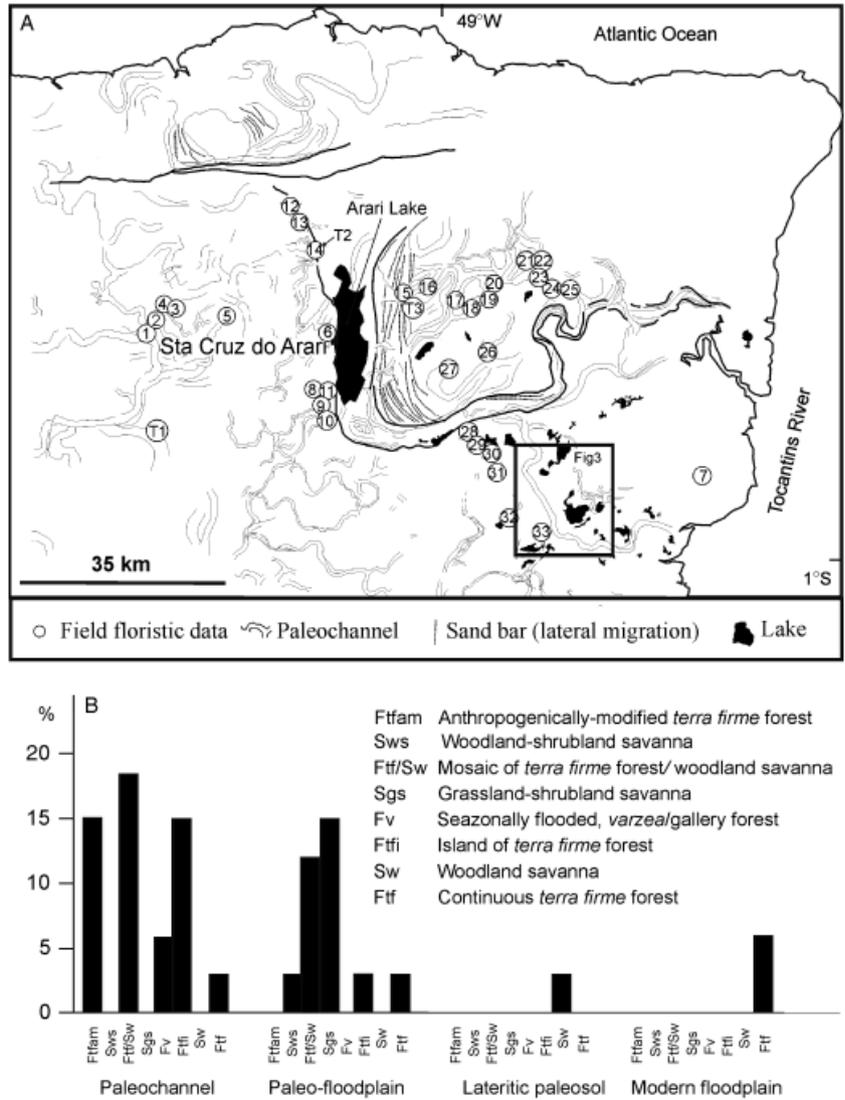
Fig. 2. (a) Map of paleochannels in eastern Marajó Island, with location of the sites where vegetation types were characterized (1-33). Note location of drill cores T1 to T4, illustrated in Figs. 6 and 7 (Inside box locates Fig. 3). **(b)** Distribution of vegetation patterns with respect to past and modern depositional environments. The *Y* axis represents the percentage of vegetation types within the 33 investigated sites.

Ten samples of sediment units were collected for radiocarbon analyses at the Beta Analytic Radiocarbon Dating Laboratory (Florida, USA), by accelerator mass spectrometer (AMS). Seven samples derive from the three sedimentological cores and three from the two cores collected for carbon isotope studies. Samples were pre-treated with acid to remove carbonates and weaken organic bonds, washed with alkali to remove secondary organic acids, and then combined with acid again to provide more accurate dating. Conventional ^{14}C ages were calibrated to calendar years using the Pretoria Calibration Procedure program, based on tree-ring data as calibration curves (Talma & Vogel 1993).

Results

Floristic analysis and terrain characterization

Characterization of vegetation types in the 33 sites (Fig. 2) revealed periodically inundated areas with savanna, and numerous elongated and sinuous belts with either savanna or various types of arboreal vegetation. A total of 174 plant species were recorded (Appendix S1) and grouped into the following life forms: tree (81 spp., 46.55%), herb (59 spp., 39.90%), liana (11 spp., 6.32%), shrub (9 spp., 5.17%), palm (7 spp., 4.02%) and epiphyte (7 spp., 4.02%) (Table 1).

Table 1. Frequency, absolute (*n*) and relative (%) species richness of plant forms studied in Marajó Island.

| Vegetation type	Number of Species	Shrub % (*n*)	Tree % (*n*)	Liana % (*n*)	Epiphyte % (*n*)	Herb % (*n*)	Stem % (*n*)	Species Richness	
								Abs (*n*)	Rel (%)
Seasonally flooded *varzea*/gallery forest (Fv)	53	18.84 (13)	13.71 (17)	22.22 (6)	100.00 (1)	18.29 (15)	7.69 (1)	53	16.77
Anthropogenically modified *terra-firme* (Ftfam).	73	23.19 (16)	27.42 (34)	18.52 (5)	(0) 0.00	15.85 (13)	38.46 (5)	73	23.10
Continuous *terra-firme* forest (Ftf)	23	8.70 (6)	7.26 (9)	7.41 (2)	(0) 0.00	4.88 (4)	15.38 (2)	23	7.28
Island of *terra-firme* forest (Ftfi)	64	20.29 (14)	27.42 (34)	14.81 (4)	(0) 0.00	12.20 (10)	15.38 (2)	64	20.25
Mosaic of *terra-firme* forest and woodland savanna (Ftf/Sw)	43	15.94 (11)	11.29 (14)	22.22 (6)	0,00 (0)	12.20 (10)	15.38 (2)	43	13.61
Woodland–shrubland savannas (Sws)	13	1.45 (1)	1,61 (2)	0.00 (0)	0.00 (0)	12.20 (10)	0.00 (0)	13	4.11
Grassland–shrubland savanna (Sgs)	27	10.14 (7)	3.23 (4)	0.00 (0)	0.00 (0)	18.29 (15)	7.69 (1)	27	8.54
Woodland savanna (Sw)	20	1.45 (1)	8.06 (10)	14.81 (4)	0.00 (0)	6.10 (5)	0.00 (0)	20	6.33

Table 2. Relationship between type of environment and plant physiognomy for each site, with indication of number of species/site (see Fig. 2b for legend of plant categories).

Environment	Vegetation type/site (number of species)							
	Fv	Ftfam	Ftf	Ftfi	Ftf/Sw	Sws	Sgs	Sw
Sandy paleochannel slightly higher than surrounding plains (Holocene)	12 (27) 32 (8)	1 (38) 4 (15) 13 (25) 18 (14)	24 (2) 31 (17)	14 (17) 16 (18) 19 (13) 30 (24) 33 (14)	9 (12) 20 (21) 21 (5) 22 (13) 23 (5) 29 (4)			
Sandy mud plain (Holocene)						2 (11) 3 (3)	17 (4)	
Mud plain (Holocene)							5 (8) 6 (11) 8 (13)	
Iron-cemented sand on Miocene lateritic paleosol								7 (21)
Mud at the margin of modern active channel	10 (19) 11 (17)							
Heterolithic (sand/mud) paleochannel slightly higher than surrounding plains (Holocene)			25 (7)	15 (22) 27 (18)	26 (13) 28 (10)			

The highest absolute and relative species richness (Table 1) was recorded for anthropogenically-modified *terra-firme* forest (Ftfam) (*n* = 73; 23.10%), followed by islands of *terra-firme* forest (Ftfi) (*n* = 64; 20.25%). Vegetation types with the lowest species diversity are woodland-shrub savanna (Sws) (*n* = 13; 4.11%) and woodland savanna (Sw) (*n* = 20; 6.33%). The majority of the belts with forest (i.e. vegetation types Fv, Ftfam, Ftf, Ftfi, Sws and Sw) is related to paleochannels (Table 2; Fig. 3a and b) and, to a lesser extent, abandoned bars. Grassland-shrubland savannas (Sgs) are widespread on flat and slightly low-lying paleofloodplains, although they also occur discontinuously over paleochannel areas. Mosaics of *terra-firme* forest and woodland savanna (Ftf/Sw) are found on both deposits. Contact between plant types is either sharp or progressive. Paleochannels with arboreal vegetation consist of elongated, sinuous to anastomosing features up to 1.2-km wide (average 0.6 to 0.9 km; Figs. 2, 3a and b). DEM analysis suggests that the paleochannels stand slightly higher relative to adjacent areas (Fig. 3b and c). Fieldwork revealed that this is mostly due to combination of tree canopy and smooth terrain elevation of a few tens of centimeters up to 2-3 m.

The paleochannels record different phases of development ranging from fully abandoned, with a
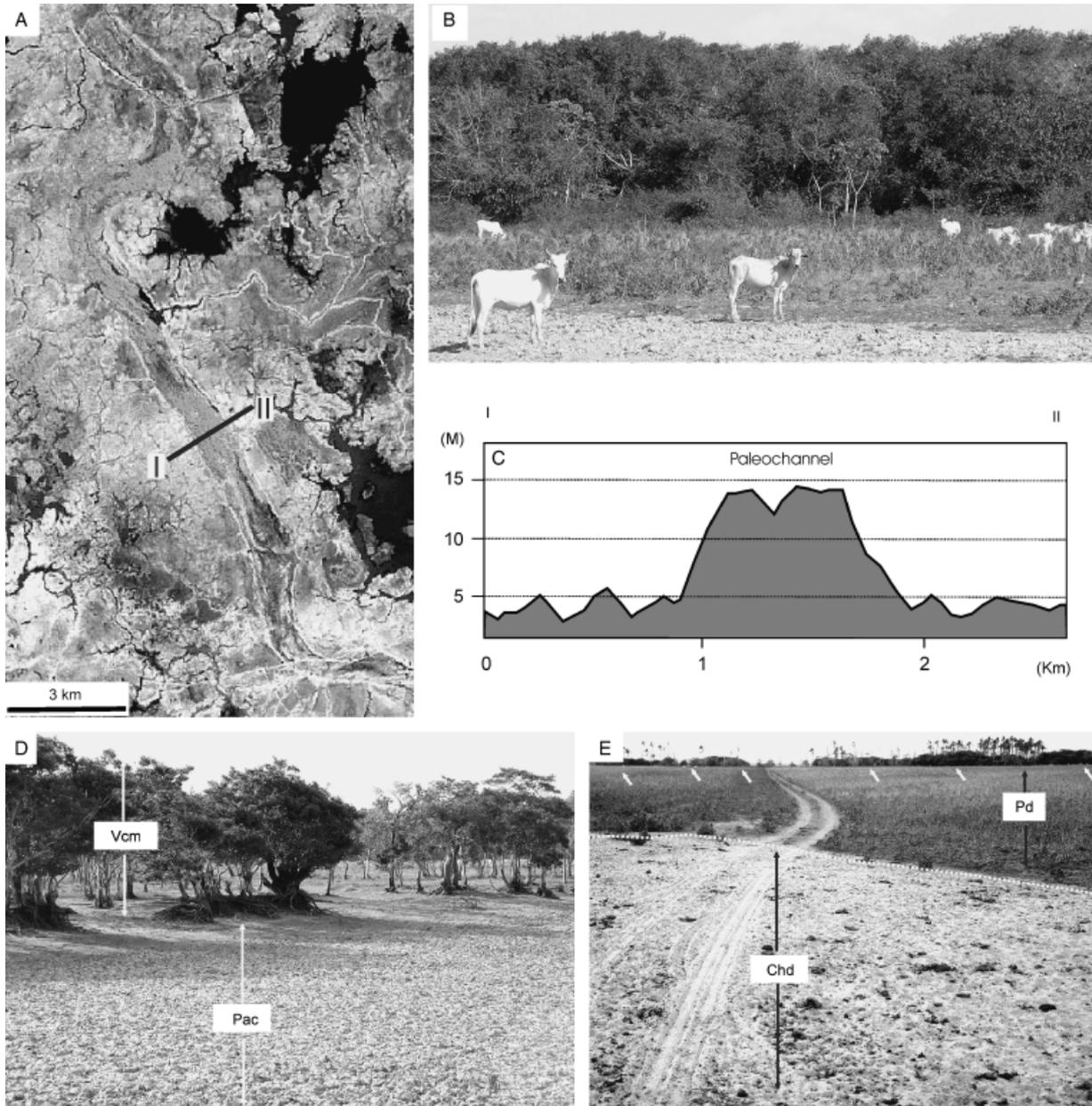
Fig. 3. Characterization of paleochannels in eastern Marajó Island. (**a**) Landsat-TM, 4(R), 5(G) and 7(B) composition illustrating a main west-northwest oriented, meandering paleochannel. (**b**) Detail of a paleochannel area covered by typical wet lowland forest. (**c**) Topographic profile transverse to the paleochannel (see profile I-II in A for location) with data obtained from SRTM-DEM. (**d**) Partly abandoned channel (Pac) with a slight concave profile. Vegetation at the channel margin (Vcm) with seasonally flooded, *varzea*/gallery forest (Fv) elements is stressed and dying due to the lack of permanent water. (**e**) Sharp contact between non-vegetated sandy paleochannel deposits (Chd) and muddy surrounding flat grassland areas (Pd) (paleochannel deposits diagonal to the picture). Note also a narrow and long belt of trees developed in a slightly parallel paleochannel (background arrows).

typical convex-up topography, to partly abandoned, with a noticeable smooth depression, although water runoff was cut off. In the latter, relics of seasonally flooded, *varzea*-gallery trees are still present, but they are sparsely distributed around the channel margins, and many have partly or entirely lost their leaves (Fig. 3d). This evidences stress due to lack of permanent flows within channels, which are now almost completely filled with sediments. Alternatively, channel morphology is either covered by vegetation (usually wet lowland forests and, less commonly, savanna) or vegetation is absent, in

which case the topmost sandy sediment is exposed to the surface. A sharp contact exists between inner and outer channel areas (Fig. 3e).

Cores from paleochannels display sand successions that grade upward into sand and mud interbeddings (Fig. 4), recording typical channel filling followed by abandonment. Radiocarbon ages (Fig. 4) indicate deposition in the latest Pleistocene and Holocene. Non-forested floodplain areas are composed of mud packages up to 22 m thick (Fig. 5a and b). These might be interbedded with streaks and discontinuous laminae or packages <0.5-m thick of very fine-grained sands. Radiocarbon ages (Figs. 4 and 5) range from 7900 ($\pm$40) ^{14}C years BP at depths of 12 m up to 3960 ($\pm$40) ^{14}C years BP only 2 m from the surface.
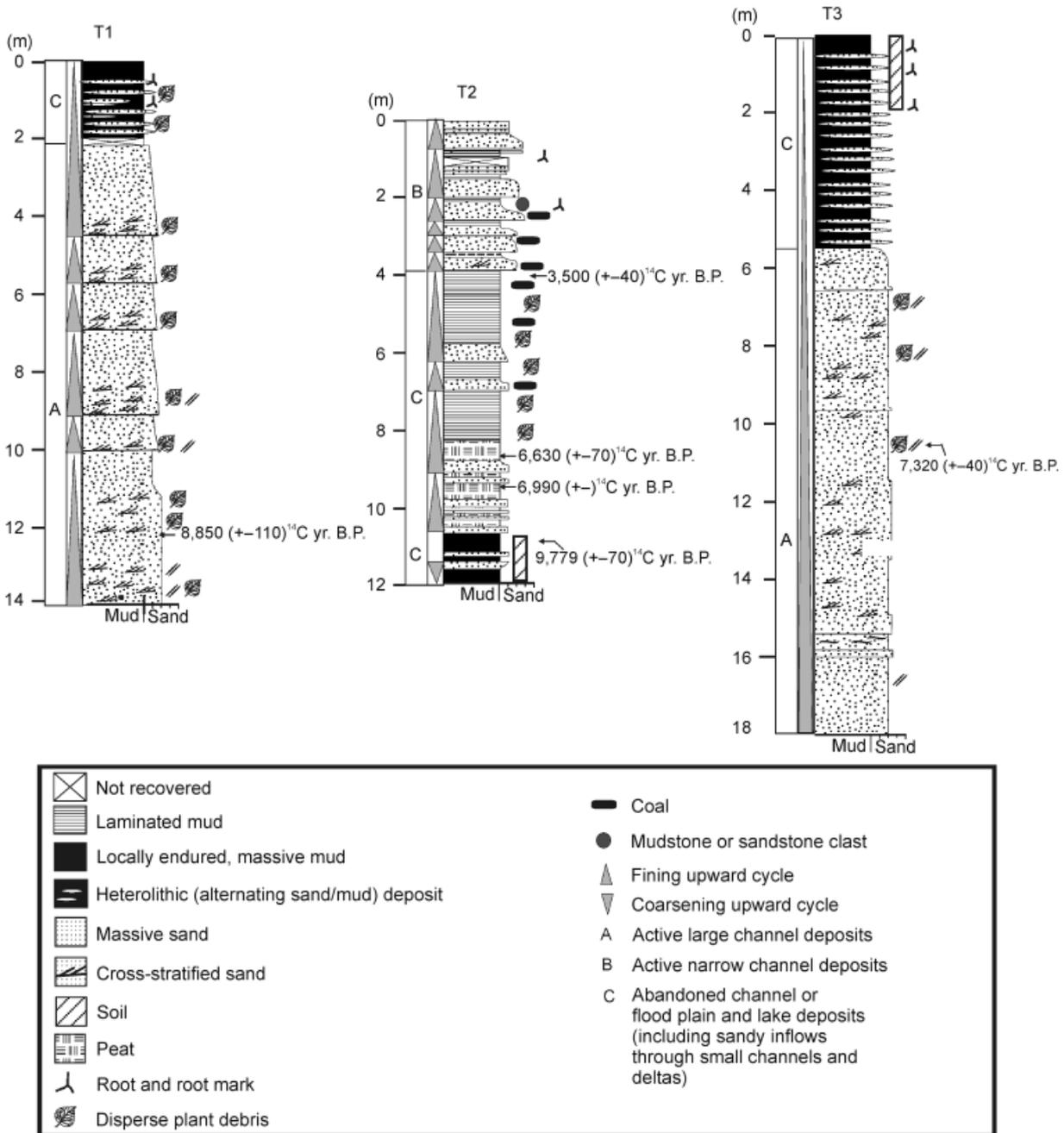
Fig. 4. Lithostratigraphic profiles from cores obtained in paleochannel areas (see Fig. 2 for location of drill cores T1 to T3). A few radiocarbon ages also plotted in these profiles indicate an early Holocene age.
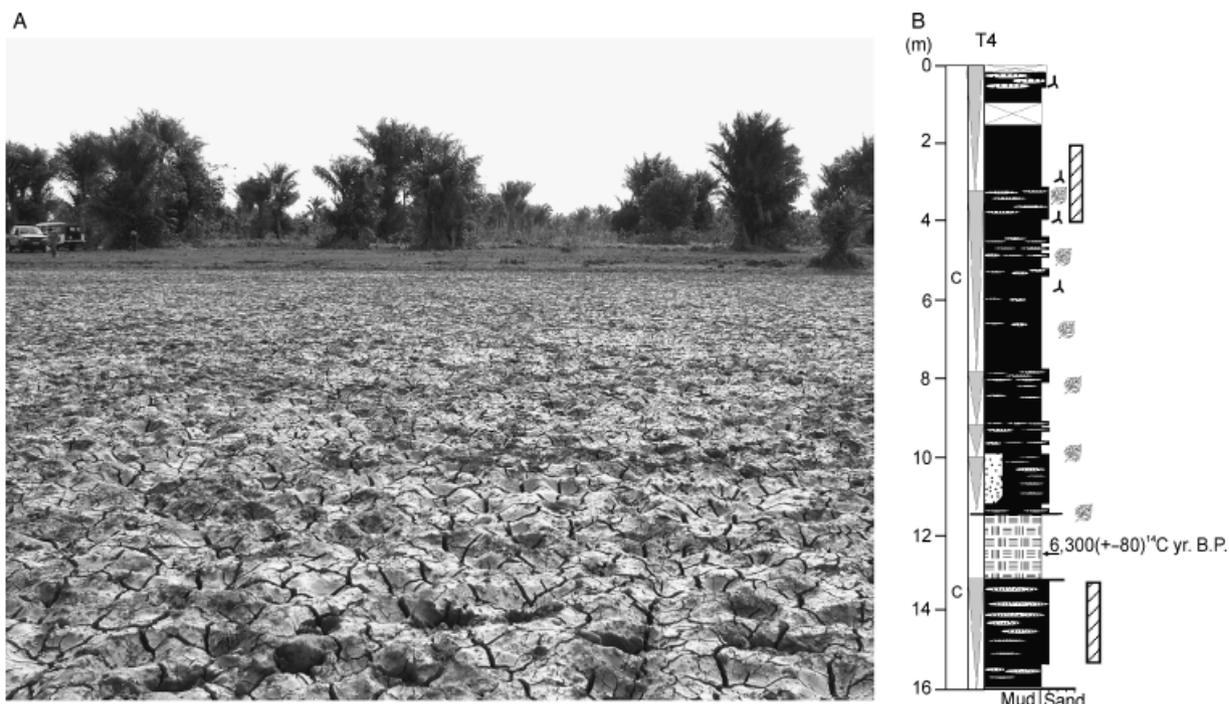
Fig. 5. (**a**) View of a typical non-vegetated muddy area around a paleochannel (vegetated background) from eastern Marajó Island. (**b**) An example of lithostratigraphic profile drilled in a muddy plain area. The radiocarbon age shows deposition contemporaneous to the paleochannel deposits shown in Fig. 4 (see Fig. 4 for legend).

^{14}C and δ^{13}C of organic matter from soil profiles

The selected ecotone forest-savanna used for studying δ^{13}C of organic matter comes from the west side of the study area (see locations 1, 3 and 4 in Fig. 2). In forested paleochannel areas (localities 1 and 4), 11 dominant plant species had the following δ^{13}C values: *Aniba citrifolia* (-33.1‰), *Cordia tetrandra* (-29.2‰), *Desmoncus polyacanthos* (-36.5‰), *Maquira coriaceous* (-32.6‰), *Anemopaegma chrysoleucum* (-31.5‰), *Parinari excelsa* (-32.3‰), *Psychotria racemosa* (-31.7‰), *Pterocarpus amazonicus* (-32.2‰) and *Simaba multiflora* (-29.9‰), and the herbs *Heliconia psitacorum* -32.9‰ and *Bambusa* sp (-27.1‰). The grass species *Panicum laxum* (-27.7‰) and *Panicum millegrana* (-30.4‰) and the shrub *Senna reticulata* (-28.9‰) were the dominant plants in the savanna vegetation located near the paleochannel area (locality 3).

The results of δ^{13}C of organic matter representative of forest (localities 1 and 4) and savanna (locality 3), as well as the radiocarbon ages for these profiles, are shown in Fig. 6. The values indicate an upward isotopic depletion in the forested areas, with a gradual enrichment (i.e. up to -18.5‰) from 2.20 to 0.70 m in locality 4. In the

savanna area, there is an upward enrichment in the values up to 1.0-m depth, followed by depletion near the surface. Radiocarbon dating obtained from locality 1 provided only late Pleistocene and Holocene ages.

Discussion

One of the major problems to evaluate environmental influence on the distribution of Amazonian plant species is the lack of geological and geomorphological information. Available low-resolution maps, in general provided at a scale of 1:1 000 000, are far from adequate to approach the main factors controlling species distribution. Floristic survey integrated with terrain characterization helps to discuss the controls on plant distribution in Marajó Island. The coexistence of large areas of savanna and wet lowland forest has not yet been discussed. Other savanna patches in Amazonia (e.g. Takeuchi 1960; Sanaiotti et al. 2002) have been related to either modern climate changes at a local scale or relics of dry vegetation from the glacial episodes (Ledru et al. 2006).

An alternative model is proposed considering the geological history. An important point to be
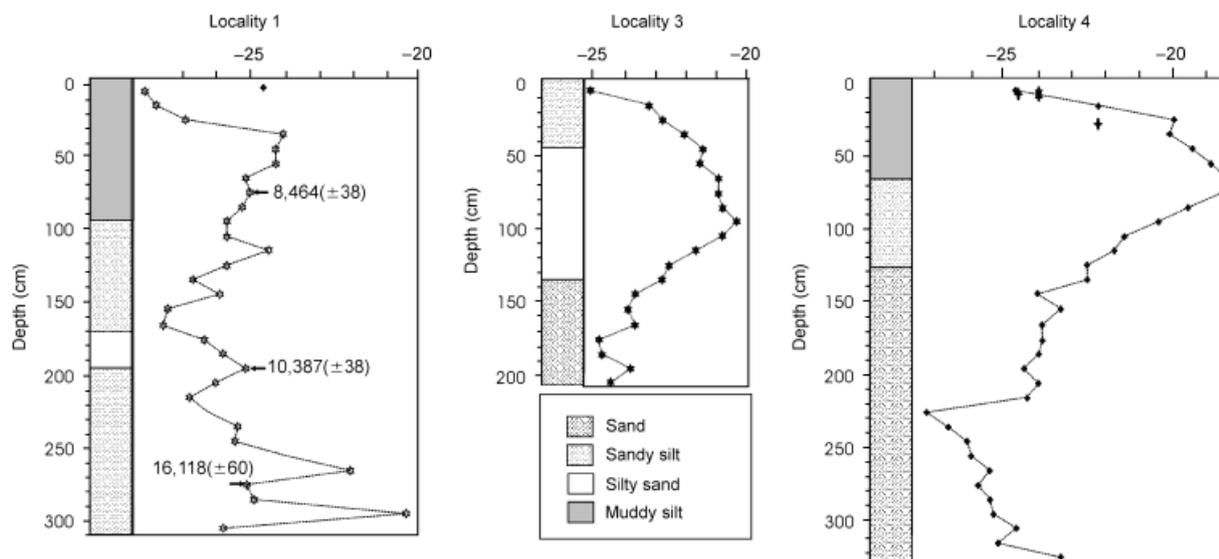
Fig. 6. δ^{13}C values (‰) of organic matter from soils in relation to depth (corresponding to localities 1, 3 and 4 in Fig. 2).

discussed is the sharp contrasts in vegetation form from forested to non-forested areas in the centre of the island. Eastern Marajó Island is dominated by savanna because a great part of its surface remains submerged during most of the year. The increased water accumulation on this side of the island reflects its lower elevation due to slight subsidence. The sharp contact between forest and savanna occurs along a major NW-SE to NNW-SSE fault zone re-activated during the latest Quaternary (Rossetti et al. 2007). A number of other studies have addressed the importance of tectonics in the latest Tertiary and Quaternary in Marajó Island (e.g. Costa et al. 2001; Rossetti & Valeriano 2007). Following subsidence, eastern Marajó Island progressively stabilized, promoting a complex history of channel/bar estab-lishment and abandonment (Rossetti et al. 2008). As discussed below, and also documented elsewhere in South America (e.g. Sarmiento & Pinillos 2001), the dynamic evolution of these landforms controlled a set of interrelated parameters (i.e. soil type, topography, hydrology) that guided plant distribution in eastern Marajó Island.

There are several studies in the literature relat-ing contrasts in plant distribution to nutrient content (e.g. Tuomisto et al. 1995; Coudun et al. 2006). Although this factor cannot be ruled out in eastern Marajó Island without undertaking further studies focusing on soil minerals, base content at root reach and soluble nutrient concentrations, the distribution of forest and savanna seems to respond to other influences. Areas of abandoned channels and bars have a sandy quartzose composition, while

surrounding areas are mostly muddy. Taking into account only these lithological compositions, more fertile soils could have been favoured on the muddy areas due to their high chemical nutrient content (i.e. Mg, K, Ca, Fe from clays) that contrasts with the Si-dominated quartzose sands from pa-leochannel areas. However, there is an overall consensus among pedologists that chemical compo-sition is rarely the main factor determining soil fertility. In fact, the paleochannels have latosols, while hydromorphic gleysols and podzols dominate the surrounding areas. These are typically nutrient-poor soils, with the two latter types been highly restrictive to the development of deep-rooted plants due to their development on muddy, water-saturated environments. Rather than reflecting che-mical availability, these soil types respond to a combination of factors, which mostly include sedi-ment texture, topography and water content. As discussed in detail below, these factors are highly dependent on landform evolution through time in eastern Marajó.

Topography, type of sub-surface water and the history of drainage abandonment had crucial roles in tree growth in eastern Marajó Island, as also documented in other Amazonian areas (e.g. Mertes et al. 1995). This is suggested by the fact that forests are, in general, related to paleochannel and bar de-posits with smooth topographies. Abandoned bars naturally stand above adjacent areas. Paleochannels might have adopted a slightly positive topography due to marginal levees, added to the fact that in-channel sands are less liable to compaction, relative
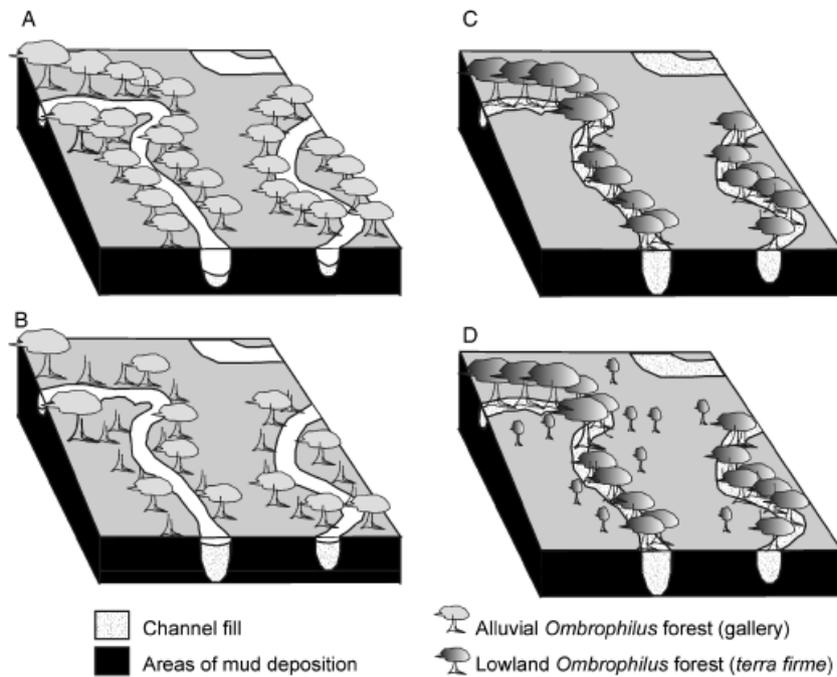
Fig. 7. Proposed model for the origin of vegetation types in eastern Marajó Island. (**a**) Deposition of sand and mud within channels and surrounding areas, respectively. (**b**) As the channel flow decreased in energy, the channels became progressively shallower and eventually abandoned. Decreasing flows caused great stress on gallery vegetation, which was replaced by savanna (not depicted). (**c**) Savannas were progressively replaced by *terra-firme* forest, with species derived from forested areas. d. Continuity of this process might amplify the forest from paleochannels over surrounding areas.

to more malleable clay layers from nearby unconfined depositional settings (Porsani 1981). Although smooth, these topographies are responsible for protecting some areas from the effect of prolonged flooding, which favours *terra-firme* forests. Many previous works have highlighted the importance of topography on the differentiation of plant species in Amazonia (e.g. Tuomisto et al. 1995; Vormisto et al. 2004).

The type of sub-surface water might have been another factor influencing tree growth in the study area. A geophysical investigation indicates that sands from paleochannel and bar deposits contain freshwater captured from either rain or running flows during wet seasons, while mud sealing precludes surface freshwater penetration down through muddy deposits in the surrounding flat areas (Porsani 1981). As a result, the latter have connate brackish to saline waters, constituting stressed environments that are unsuitable for the growth of *varzea* and *terra-firme* forests. Similar controls on vegetation growth dictated by groundwater salinity driven by river dynamics are recorded in the literature (e.g. Thevs et al. 2008a).

In combination with the factors above, the history of channel abandonment additionally

contributed to different plant groups in eastern Marajó Island. The proposed model considers that the slack running water during channel abandonment led to the disappearance of *varzea*/gallery forest at channel margins. The occurrence of many modern channels in process of abandonment with decaying gallery forests (Fig. 7b) inspired this model. When channels are fully abandoned and filled with sediment, the channel surface is occupied first by grasslands and ultimately by *terra-firme* forests (Fig. 7a–c). First, island and mosaics of *terra-firme* and savanna are established over confined, sinuous channel morphologies, then the forest expands beyond the channel limits through time, resulting in more continuous areas with *terra-firme* forest (Fig. 7c). This model is consistent with the fact that continuous *terra-firme* forest shares the highest number of taxa with islands of *terra-firme* forest and mosaics of *terra-firme* forest and savanna, supporting that the latter are in the process of development, benefiting from species migration from adjacent forests. The transitional zone between forested paleochannels and nearby grassland areas might be evidence that arboreal species present in the latter are migrating towards savanna areas (Fig. 7d). Thus, channels abandoned for longer times sustain

better-structured vegetation, represented by continuous *terra-firme* forests, because they had more time for a larger number of tree species to arrive and become established. On the other hand, channels abandoned later, i.e. more recently, have not yet had time to become sites for widespread development of plant species.

Stable carbon isotope composition ($\delta^{13}C$) of soil organic matter can be used to further support the above proposed model. Hence, the $\delta^{13}C$ values display fairly comparable patterns in all analysed cores, independent of their locations in forest or savanna. The three profiles suggest C_3 plants at ∼16,000 years BP. This type of vegetation remained constant in locality 1, in a forested area. However, in the other forested locality analysed in this study (i.e. locality 4), carbon isotope enrichment at ∼6000 years BP suggests a significant influence of C_4 plants, which might be related to expansion of savanna over forest. The isotopic depletion after ∼6000 years BP records the moment when dense arboreal vegetation returned to this site. The similar isotopic enrichment recorded in the savanna site (profile 3) also suggests an opening of vegetation (mixture of C_3 and C_4 plants). Upward to the shallow layer, the values gradually become more depleted ($-23.9‰$), suggesting denser (arboreal) vegetation and/or more significant presence of C_3 grasses. Several authors (including some of the present ones) have related changes in vegetation pattern in the Quaternary of Amazonia to climate fluctuations (e.g. Pessenda et al. 1998; Behling & Hooghiemstra 2000; Mayle et al. 2000). Considering this interpretation, the upward transition from arboreal to savanna, and then to arboreal and/or C_3 grasses, could be related to a transition from humid to drier climates, and then back to the modern humid condition. Despite an equitable climate, the coexistence of forest and savanna at the Present leads to the introduction of an alternative model to explain vegetation patterns in eastern Marajó Island.

The dominance of arboreal vegetation surrounding areas with paleochannels, as indicated mainly in site 4 by the depleted $\delta^{13}C$ values at deeper layers, could be related to a swampy landscape, when large channels were active, probably with gallery forests. The gallery trees gradually changed to C_4 grasses, pointing to savanna expansion, which, according to the above model, could reflect decreasing flows, followed by channel abandonment. As the channels were completely abandoned and filled with sandy and silty sediments, they became sites of arboreal vegetation. The gradual upward increase of the C_3 plant signal in the organic matter of pa-

leochannel deposits (localities 1 and 4) is consistent with this interpretation. C_3 plants expanded toward interchannel areas, mixing with C_4 grasses, which resulted in depletion of $\delta^{13}C$ values in the upper portions of profiles 3 and 4.

Final Remarks

Eastern Marajó Island might have had even more widespread, non-vegetated or open-vegetated areas than today at the time the channels were active, i.e. in latest Pleistocene and early Holocene. As the channels became progressively abandoned, they were filled with sediments, mostly sands. The sand bodies acted as freshwater reservoirs, and also stood slightly higher in the landscape, eventually remaining above water level even during rainy seasons, configuring substrates favourable for tree growth. Channels abandoned longer ago have more dense forest cover than channels abandoned more recently. If this model is correct, than one can state that areas with open vegetation in eastern Marajó have decreased in size since the channels were active. As these features become progressively abandoned, there has been invasion of arboreal species, probably derived from the western side of the island. Considering the continuity of this process, one could predict that the wet lowland forest that dominates to the west will amplify eastwards in the near future.

This paper helps to further support the limitation of climatic parameters in models aiming to analyse Amazonian biodiversity. As illustrated herein, the modern landforms have strongly influenced the distribution of flooded and non-flooded areas in Marajó Island, determining the location of the various vegetation types. This study should drive further investigation focusing on vegetation distribution in other Amazonian areas, where fault reactivation during the Tertiary and Quaternary has also modified the landscape, changing the course of many rivers. Therefore, together with climate, modelling exercises focusing on Amazonian biodiversity can greatly benefit from the inclusion of a geological history perspective into databases, a task that can only be undertaken with the establishment of research groups having an interdisciplinary approach.

and Carlos A. Silva for help with the floristic survey. The several comments and corrections made by three anonymous reviewers and the Coordinating Editor, Dr. Valerio Pillar, significantly improved the first version of the manuscript.

References

Ayres, J.M. & Clutton-Brock, T.H. 1992. River boundaries and species range size in Amazonian primates. *American Nature* 140: 531–537.

Anon (Radam.) 1974. Folha SA.22 Belém. Departamento Nacional de Produção Mineral, Rio de Janeiro, BR.

Anon (USDA, Soil Survey Staff.) 1999. Soil taxonomy. A basic system of soil classification for making and interpreting soil surveys. 2nd edn. USDA-NRCS Agric. Handb., US Government Printing Office, Washington, DC, US, 436 pp.

Bastos, M.N.C. 1984. Levantamento florístico do Estado do Pará. I. Campos de Joanes (Ilha do Marajó). *Boletim do Museu Paraense Emílio Goeldi (Série Botânica)* 1: 67–86.

Behling, H. & Hooghiemstra, H. 2000. Holocene Amazon rainforest–savanna dynamics and climatic implications: high resolution pollen record from Laguna Loma Linda in eastern Colombia. *Journal of Quaternary Science* 15: 687–695.

Bonaccorso, E., Koch, I. & Peterson, A.T. 2006. Pleistocene fragmentation of Amazonian species' range. *Diversity and Distributions* 12: 157–164.

Bush, M.B. 1994. Amazonian speciation: a necessary complex model. *Journal of Biogeography* 21: 5–17.

Costa, J.B.S.C., Bemerguy, R.L., Hasui, Y. & Borges, M.S. 2001. Tectonics and paleogeography along the Amazon River. *Journal of South American Earth Sciences* 14: 335–347.

Coudun, C., Gégout, J.-C., Piedallu, C. & Rameau, J.-C. 2006. Soil nutritional factors improve models of plant species distribution: an illustration with *Acer campestre* (L.) in France. *Journal of Biogeography* 33: 1750–1763.

Cronquist, A. 1981. *An integrated system of classification of flowering plants*. Columbia University Press, New York, NY, US, 1261pp.

Freitas, H.A., Pessenda, L.C.R., Aravena, R., Gouveia, S.E.M., Ribeiro, A.S. & Boulet, R. 2001. Quaternary Vegetation Dynamics in the Southern Amazon Basin Inferred from Carbon Isotopes in Soil Organic Matter. *Quarternary Research* 55: 39–46.

Haffer, J. 1990. Avian species richness in tropical South America. *Studies on Neotropical Fauna and Environment* 25: 157–183.

Henderson, A., Beck, H.T. & Scariot, A. 1991. Flora de palmeiras da Ilha de Marajó, Pará, Brasil. *Boletim do Museu Paraense Emílio Goeldi (Série Botânica)* 7: 199–222.

Huntley, B., Green, R.E., Collingham, Y.C., Hill, J.K., Willis, S.G., Bartlein, P.J., Cramer, W., Hagemeijer, W.J.M. & Thomas, C.J. 2004. The performance of models relating species geographical distributions to climate is independent of trophic level. *Ecology Letters* 7: 417–426.

Ledru, M.-P., Ceccantini, G., Gouveia, S.E.M., López-Sáez, J.A., Pessenda, L.C.R. & Riberito, A.S. 2006. Millennial-scale climatic and vegetation changes in a northern Cerrado (Northeast, Brazil) since the last glacial maximum. *Quaternary Science Reviews* 25: 1110–1126.

Mayle, F.A., Burbridge, R. & Killeen, T.J. 2000. Millennial-scale dynamics of southern Amazonian rain forests. *Science* 290: 2291–2294.

McCune, B. & Mefford, M.J. 1997. *PC-ORD for windows: multivariate analysis of ecological data – verson 3.12.* MJM Software Design, Gleneden Beach, OR, US.

Mertes, L.A.K., Daniel, D.L., Melack, J.M., Nelson, B., Marinelli, L.A. & Forsberg, B.R. 1995. Spatial patterns of hydrology, geomorphology, and vegetation on the floodplain of the Amazon River in Brazil from a remote sensing perspective. *Geomorphology* 13: 215–232.

Miranda, I.S. & Carneiro, A. 1994. Similaridade florística de algumas savanas amazônicas. *Boletim do Museu Paraense Emílio Goeldi (Série Botânica)* 10: 249–267.

Pearson, R.G. & Dawson, T.P. 2003. Predicting the impacts of climate change on the distribution of species: are bioclimate envelope models useful? *Global Ecology and Biogeography* 12: 361–371.

Pessenda, L.C.R., Valencia, E.P.E., Camargo, P.B., Telles, E.C.C., Martinelli, L.A., Cerri, C.C., Aravena, R. & Rozanski, K. 1996. Natural radiocarbon measurements in Brazilian soils developed on basic rocks. *Radiocarbon* 38: 203–208.

Pessenda, L.C.R., Gomes, B.M., Aravena, R., Ribeiro, A.S., Boulet, R. & Gouveia, S.E.M. (1998). The carbon isotope record in soils along a forest–cerrado ecosystem transect: implications for vegetation changes in the Rondonia state, southwester Brazilian Amazon region. *The Holocene* 8: 599–603.

Pires, J.M. & Prance, G.T. 1985. The vegetation types of the Brazilian Amazon. In: Prance, T.E. & Lovejoy, T.E. (eds.) *Key environments: Amazonia.* pp. 109–145. Pergamon, New York, NY, US.

Porsani, M.J. 1981. Paleocanais, uma opção para prospecção de água subterrânea na Ilha de Marajó. M.Sc. Thesis, Universidade Federal do Pará, Belém, BR.

Räsänen, M.E., Salo, J.S., Jungner, H. & Romero-Pittman, L. 1990. Evolution of the Western Amazon lowland relief: impact of Andean foreland dynamics. *Terra Nova* 2: 320–332.

Rossetti, D.F. & Valeriano, M.M. 2007. Evolution of the lowest Amazon basin modeled from the integration of geological and SRTM topographic data. *Catena* 70: 253–265.

Rossetti, D.F., Góes, A.M., Valeriano, M.M. & Miranda, M.C.C. 2007. Quaternary tectonics in a passive margin: Marajó Island, northern Brazil. *Journal of Quaternary Science* 23: 121–135.

Rossetti, D.F., Valeriano, M.M., Góes, A.M. & Thalles, M. 2008. Paleodrainage in Marajó Island (northern Brazil) and its relation to Holocene relative sea-level. *The Holocene* 18: 923–934.

Sanaiotti, T.M., Martinelli, L.A., Victoria, R.L., Trumbore S, E. & Camargo, P.B. 2002. Past vegetation changes in Amazon savannas determined using carbon isotopes of soil organic matter. *Biotropica* 34: 2–16.

Sarmiento, G. & Pinillos, M. 2001. Patterns and processes in a seasonally-flooded tropical plain: the Apure Llanos, Venezuela. *Journal of Biogeography* 28: 985–996.

Sayre, R., Roca, E., Sedaghatkish, G., Young, B., Keel, S., Roca, R. & Sheppard, S. 2000. *Nature in focus: rapid ecological assessment. The nature conservancy*. Washington, DC, US.

Talma, A.S. & Vogel, J.C. 1993. A simplified approach to calibrating ^{14}C dates. *Radiocarbon* 35: 317–322.

Takeuchi, M. 1960. A estrutura da vegetação na Amazônia. II - As savanas do Norte da Amazônia. *Boletim do Museu Paraense Emilio Goeldi* 7: 3–14.

ter Steege, H., Pitman, N., Sabatier, D., Castellanos, H., Van Der Hout, P., Daly, D.C., Silveira, M., Phillips, O., Vasquez, R., Van Andel, T., Duivenvoorden, J., Oliveira, A.A., Ek, R., Lilwah, R., Thomas, R., Van Essen, J., Baider, C., Maas, P., Mori, S., Terborgh, J., Vargas, P.N., Mogollón, H. & Morawetz, W. 2003. A spatial model of tree-diversity and -density for the Amazon Region. *Biodiversity Conservation* 12: 2255–2276.

Thevs, N., Zerbe, S., Peper, J. & Succow, M. 2008a. Vegetation and vegetation dynamics in the Tarim River floodplain of continental-arid Xinjiang, NE China. *Phytocoenologia* 38: 65–84.

Tuomisto, H. & Ruokolainen, K. 1994. Distribution of Pteridophyta and Melastomataceae along an edaphic gradient in an Amazonian rain forest. *Journal of Vegetation Science* 5: 25–34.

Tuomisto, H., Ruokolainen, K., Kalliola, R., Linna, A., Danjoy, W. & Rodriguez, Z. 1995. Dissecting Amazonian biodiversity. *Science* 269: 63–66.

Van der Hammen, T., Duivenvoorden, J.F., Lips, J.M., Urrego, L.E. & Espejo, N. 1992. The late quaternary of the middle Caquetá area (Colombian Amazonia). *Journal of Quaternary Sciences* 7: 45–45.

Vormisto, J., Tuomisto, H. & Oksanen, T. 2004. Palm distribution patterns in Amazonian rainforests: what is the role of topographic variation? *Journal of Vegetation Science* 15: 485–494.

Supporting Information

Additional Supporting Information may be found in the online version of this article:

Appendix S1. Distribution of species occurrence in the studied sites of eastern Marajó Island (see Fig. 2b for legend of vegetation types and Fig. 2a for site location). (0 = absent; 1 = occasional or rare; 2 = common; 3 = abundant).

Please note: Blackwell Publishing are not responsible for the content or functionality of any supporting materials supplied by the authors. Any queries (other than missing material) should be directed to the corresponding author for the article.